Volume 50 | Number 63 | 14 August 2014 | Pages 8611–8802

ChemComm

Chemical Communications

www.rsc.org/chemcomm

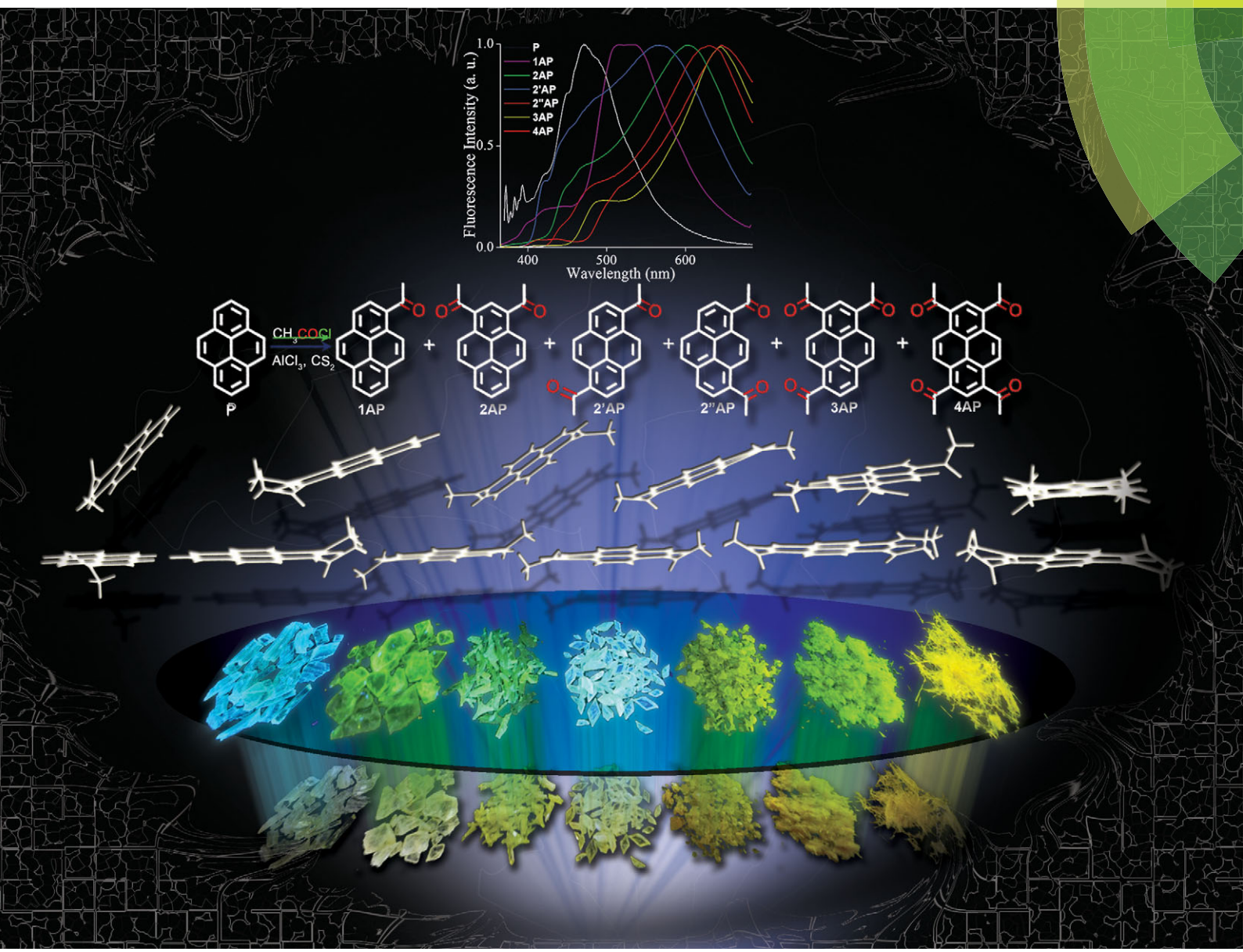

ISSN 1359-7345

ROYAL SOCIETY OF CHEMISTRY

COMMUNICATION

Mahesh Hariharan *et al.*

Progressive acylation of pyrene engineers solid state packing and colour *via* C–H···H–C, C–H···O and π–π interactions

ChemComm

COMMUNICATION

View Article Online
View Journal | View Issue

Progressive acylation of pyrene engineers solid state packing and colour *via* C–H···H–C, C–H···O and π–π interactions†

Cite this: *Chem. Commun.*, 2014, 50, 8644

Received 13th March 2014,
Accepted 9th May 2014

DOI: 10.1039/c4cc01897d

www.rsc.org/chemcomm

Shinaj K. Rajagopal, Abbey M. Philip, Kalaivanan Nagarajan and Mahesh Hariharan*

Quantum theory of atoms-in-molecules and Hirshfeld surface analyses indicated an increase in the extent of (i) C–H···H–C; (ii) C–H···O, (iii) π–π interactions and a decrease in the extent of (i) σ–π interaction, (ii) an interplanar angle between the vicinal pyrene units in a series of acetylpyrene derivatives offering blue–green–orange emissive crystals.

Molecular crystal engineering[1] of polyaromatic hydrocarbons to yield 1–2D lamellar arrangement demonstrated a pivotal role in photonic[2] and semiconductor device applications.[3] Extended orbital overlap through π-columnar stacks compared to a herringbone arrangement of arenes proved to be vital.[4] Recent efforts in transforming the herringbone to the columnar arrangement of arenes through various methods such as chemical modifications,[5] co-[6] and solvent-crystallization,[7] heat-mode,[8] mechanical stimulation[9] and solid seeding[10] have proven to be effective. Achieving a diverse degree of orbital overlap between the neighboring units in the crystalline state is still a challenging task. Monitoring the effect of subtle orientation differences and thereby the orbital overlap between the neighboring units in arenes is even more challenging. The extent of orbital overlap through π–π interactions between the vicinal arenes could be reflected in the optical properties of the crystals.[11] Extremely high sensitivity of pyrene fluorescence towards environmental effects can amplify the consequence of orientation factor/orbital overlap between the adjacent units.[12]

Our ongoing interest to regulate the arene–arene interactions in fluorescent crystals,[13] vesicular gels[14] and thin films prompted us to explore the correlation between optical properties *vs.* peripheral substitution of pyrene. We employed a simple and convenient Friedel–Crafts reaction, invented 137 years ago,[15] to increase the number of carbonyl groups in pyrene. Carbonyl conjugated arenes in solution exhibit diverse excited state processes[16] depending on the adjacent functionality such as (i) low fluorescent ($\Phi_f < 0.002$) aryl aldehydes/ketones dominated by intersystem crossing (ISC); (ii) moderate fluorescent secondary/tertiary carboxamides[17] dominated by internal conversion and (iii) high fluorescent aryl acids/esters[18] dominated by radiative processes. Extremely low Φ_f in solution hampered the efforts to explore the optical properties of aryl ketones/aldehydes in the crystalline state though a plethora of pyrene derivatives have been explored for optoelectronic applications.[19]

Furthermore, heteropolar C–H···H–C interactions are rarely found to be an integral force in organic crystals when compared to C–H···O,[20] C–H···π,[21] homopolar C–H···H–C[22] interactions, *etc.* Heteropolar C–H···H–C interactions could arise from the dipolar/quadrupolar nature of sp^2 C–H bond that could induce a dipole on the vicinal sp^3 C–H unit. Highly electronegative substituents/groups adjacent, either geminal or vicinal, to an sp^2 C–H unit may polarize the bond allowing for extended interactions.[23] We herein report for the first time a systematic control on the organization of adjacent pyrene units through the progressive addition of acetyl groups that transform the sandwich herringbone structure of pyrene to a columnar arrangement in tri/tetraacetylpyrene. Distinct packing arrangements, through C–H···H–C, C–H···O and π–π interactions, in acetylpyrene derivatives offer diverse solid-state colouring and fluorescent properties.

Adding a stoichiometric quantity of acetyl chloride to a solution of pyrene and $AlCl_3$ in carbon disulfide (CS_2) at ambient temperature rendered the desired acetyl derivatives (**1–4AP**) with moderate yield (Scheme 1, row I).[24] Compounds (**1**, **2**, **2′**, **2″**, **3AP**) were crystallized by varying the acetone : hexane composition, whereas **4AP** was obtained by temperature gradient cooling in chloroform. Acetyl derivatives (**1**, **2′**, **2″**, **3**, **4AP**) yielded solvent free monoclinic crystal system except for **2AP** which exhibits a solvent free orthorhombic crystal system (Scheme 1, row II; Table S1, ESI†). Differential scanning calorimetric (DSC) analysis of 1-acetylpyrene (**1AP**) exhibited a sharp melting transition (T_m) at 90.4 °C (Fig. S1a, ESI†). A significant

School of Chemistry, Indian Institute of Science Education and Research Thiruvananthapuram, CET Campus, Sreekaryam, Thiruvananthapuram, Kerala, India 695016. E-mail: mahesh@iisertvm.ac.in

† Electronic supplementary information (ESI) available: Experimental details, summary of crystal structure and refinement details of **1–4AP**. CCDC 984436–984441. For ESI and crystallographic data in CIF or other electronic format see DOI: 10.1039/c4cc01897d

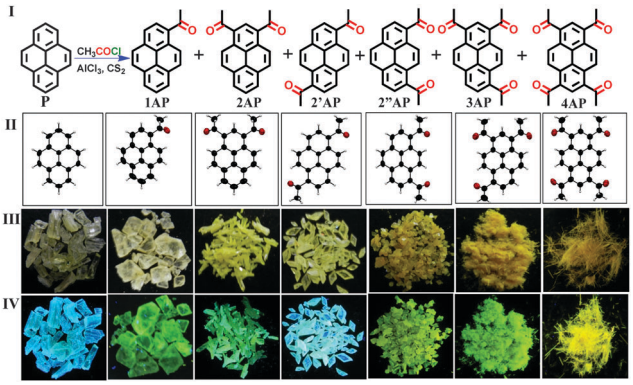

Scheme 1 Row I: molecular structure of **1–4AP**; row II: corresponding single crystal X-ray structure. Photographic image of the crystals row III: in daylight; and row IV: under UV illumination. X-ray structure of **P** is taken from the literature.[26]

decrease (*ca.* 63 °C) in the T_m of **1AP** when compared to the T_m of the model compound pyrene (**P**)[25] is indicative of attenuation in the ordered arrangement of the crystalline **1AP**. However, further increase in the number of acetyl groups in the pyrene core resulted in a near-linear increase (Fig. S1b, ESI†) in the T_m having a maximum of 295.6 °C as in the symmetric **4AP** derivative. A similar trend was observed for the change in enthalpy during the melting process for **1–4AP** (Fig. S1c and Table S2, ESI†).

Qualitative analyses of the single crystal X-ray structure of **1–4AP** indicate intra- and intermolecular distances between the methyl and aryl hydrogens in the range of 2.098–2.4 Å (Tables S3 and S4, ESI†). Distances appearing at less than the double of van der Waal's radius of hydrogen atom (2.4 Å) could indicate the existence of dihydrogen (H···H) bonding.[27] Quantum theory of atoms in molecules analyses[28] (QTAIM) of the crystalline **1–4AP** offered no characteristics supporting the intramolecular dihydrogen interactions at distances less than 2.4 Å. Intermolecular C–H···H–C interactions in crystalline **2**, **3** and **4AP** (Fig. S2, ESI†) are exemplified through the values of electron density at the (3, −1) bond critical point (BCP; $\rho_b(r)$), its Laplacian ($\nabla^2\rho_b(r)$), the interaction distance (d) as indicated in Table 1 (also see Table S4, ESI†), a bond and virial path in the potential energy density map. A closed-shell intermolecular C–H···H–C interaction possessing considerable bond path between a pair of similar hydrogens (CH_3) is seen in **2AP** (Fig. S2a, ESI†). Non polar C–H···H–C interaction evaluated accumulation of electron density, $\rho_b(\boldsymbol{r})$, 0.036 e Å^{-3} and the positive value of the Laplacian at the BCP (0.52 e Å^{-5}), to form extended chain-like C–H···H–C contacts along the *b*-axis in **2AP**. Derivatives **1**, **2′** and **2″AP** lack intermolecular C–H···H–C interaction as confirmed through QTAIM calculations.

Similar electronegativity differences between involved sp^3 C–H bonds could only arise from electrically neutral hydrogens in the vicinity. The influence of the adjacent carbonyl group may impart repulsive C–H···H–C interactions from the first order electrostatic contribution. C–H···H–C contacts could be due to second-order mutual polarization of distorted charge

Table 1 Calculated topological properties of the electron density for the intermolecular interaction in **2–4AP**

	C–H···H–C contacts	d^a (Å)	$\rho_b(\boldsymbol{r})$,^{b} (e Å^{-3})	$\nabla^2\rho_b(\boldsymbol{r})^c$ (e Å^{-5})	DE^d (kJ mol^{-1})
2AP	H18c···H′18c	2.230	0.036	0.520	3.46
3AP	H20c···H′8	2.246	0.041	0.471	4.29
	H20c···H′9	2.579^e	0.019	0.249	1.87
4AP	H′18c···H″22c	2.239	0.040	0.514	4.32
	H′4···H18a	2.394	0.034	0.450	3.50
	H′5···H18c	2.577^e	0.023	0.300	2.29

^{a} d = distance. ^{b} $\rho_b(r)$ = electron density at the BCP. ^{c} $\nabla^2\rho_b(r)$ = Laplacian of $\rho_b(r)$. ^{d} DE = dissociation energy (see ESI for details). ^{e} Though H···H distance is >2.4 Å, QTAIM exhibited electron density at (3, −1) BCP.

clouds of the C–H bonds due to the vicinal carbonyl group. Carbonyl groups adjacent to the interacting sp^3 methyl groups could make the C–H bonds both polarizable and polarizing with respect to each other, as observed for B–H bonds.[29] **3AP** exhibits (CH_3)H···H(aryl) interactions whereas **4AP** shows a bond path for (CH_3)H···H(CH_3) and (CH_3)H···H(aryl) interactions (Fig. S2b and c, ESI†). QTAIM calculations also confirmed the existence of C–H···O and C–H···C interactions in the derivatives **2–4AP**, apart from the C–H···H–C contacts (Table S4, ESI†).

Hirshfeld surface analyses[30] of **1–4AP** (Fig. 1 and Table S5, ESI†) exhibit systematic trends in the weak interactions with an increase in the number of substituted acetyl groups per pyrene unit as the following (i) decrease in the C···H contacts that corresponds to σ–π (edge-to-face) interactions; (ii) increase in the C···C contacts that corresponds to π–π (face-to-face) interactions; (iii) increase in the O···H contacts that corresponds to C–H···O interactions; (iv) increase in the H···H contacts that

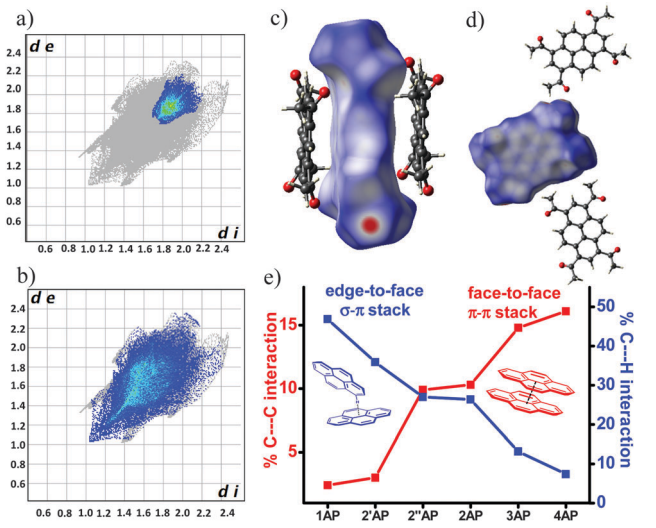

Fig. 1 Hirshfeld 2D fingerprint plot of **4AP** with the region of the plots corresponding to (a) C···C and (b) H···H interactions; Hirshfeld surface of **4AP** mapped with d_{norm} depicting (c) C···C and (d) H···H interactions; (e) percentage contribution of edge-to-face (C···H) and face-to-face (C···C) interactions in **1–4AP**.

corresponds to dihydrogen interactions and (v) increase in the O···C contacts that corresponds to dipolar interactions between the carbonyl groups. Concurrence of such weak intermolecular interactions dictates the molecular packing that results in ideal columnar 2D stacks in **4AP** having ρ = 0.46 (Fig. 2). A value of ρ = 19.5 in **1AP** indicates the formation of a herringbone structure in the crystalline lattice when compared to the sandwich herringbone structure in the **P** (ρ = 3.4). Efficient reduction in the ρ value from **1–4AP** is a consequence of simultaneous (i) decrease in the percentage of C···H contacts (σ–π stacking) from 46.9% (**1AP**) to 7.4% (**4AP**) and (ii) increase in the C···C contacts (π–π stacking) from 2.4% (**1AP**) to 16.1% (**4AP**). With an increase in the number of acetyl groups in the pyrene core, crystal packing of **1–4AP** shows distinct patterns through a gradual decrease in the interplanar angle between the adjacent pyrene units (θ = 48.4° for **1AP** and θ = 0° for **4AP**; Fig. S3 and Table S6, ESI†). Decrease in the interplanar angle was accompanied by transformation of the herringbone structure of **1AP** to the columnar structure of **4AP**. **2′AP** shows herringbone packing without π–π overlap between adjacent pyrene units while the crystal structure of **2**, **2″AP** shows a lamellar motif with 2D π–π stacking (brickwork/γ-motif). The torsional angles between the planes of adjacent pyrene units in **2**, **2″AP** were found to be 0° and 1°, respectively (Fig. S4 and S5, ESI†). **3AP** shows columnar stacks with extended 2D π–π stacking (β-motif), consistent with **4AP**. While **3AP** exhibited a torsional angle of 67.8° between the planes of adjacent pyrene units, a near-orthogonal (80.4°) arrangement of pyrene units was observed for **4AP**, consistent with the 1,3,6,8-tetraphenylpyrene derivatives reported by Geerts, Bredas and coworkers.[31] We observed a π–π stacking distance of 3.4–3.5 Å in **4AP** when compared to 4.8 Å in 1,3,6,8-tetrakis(4-methoxyphenyl)-pyrene reported earlier.[31] By virtue of the smaller size of the acetyl *vs.* phenyl substituents, we observed a shorter π–π stacking distance in **4AP**.

In **2AP**, carbonyl oxygen interacts with the aryl hydrogen (C–H···O; Fig. S6, ESI†) forming a zig-zag arrangement along the *b*-axis (out-of-plane; 1D), while **2′AP** favors a linear arrangement along the *c*-axis possessing C–H···O interactions. An interplanar angle of 14.5° between the pyrene units in **2″AP** arises from C–H···O contacts. Extended C–H···O interactions in **3–4AP** across the *ab*-plane promotes a sheet-like arrangement of pyrene units (Fig. S6, ESI†) in combination with interplanar C–H···O interactions that support the pyrene (β-structure) stacks along the *c*-axis. In addition to C–H···O interactions, we observed C–H···H–C contacts (3.46–4.32 kJ mol^{-1}; Table 1) in crystalline **2–4AP**. C–H···H–C contacts in **2AP** (*b*-axis; in-plane; 1D) and **3AP** (*a*-axis; in-plane; 1D) promote a linear arrangement of the pyrene units. In **4AP**, C–H···O interactions promote stacks along the *c*-axis which is reinforced by C–H···H–C contacts across the *ab*-plane.

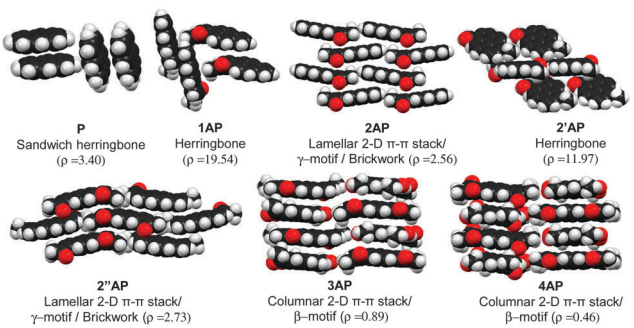

Fig. 2 Close packing arrangement in **1–4AP** indicating the values of ρ[(%C···H)/(%C···C)].[34] Herringbone (ρ > 4.5), sandwich herringbone (3.2 < ρ < 4.0), γ (1.2 < ρ < 2.7), β (0.46 < ρ < 1.0).

We performed steady-state and time-resolved photophysical measurements to correlate the extent of overlap between adjacent pyrene units *vs.* colour properties in crystalline **1–4AP**. Experiments were also carried out in dilute solutions of chloroform to understand the photophysical properties of **1–4AP**. Increasing the number of acetyl groups resulted in progressive red-shift in the UV-Vis absorption maximum of **1–4AP** in chloroform, for example 22 nm (**1AP**) and 70 nm (**4AP**), when compared to **P** (Table S7, Fig. S7a, ESI†). Upon excitation at 350 nm, the emission maximum of **1–4AP** in chloroform exhibited a similar trend indicating the role of extended conjugation arising from carbonyl group(s) in the electronic transitions in the pyrene unit (Fig. S7b, ESI†). We observed a significant decrease in the fluorescence quantum yield of **1–4AP** (Φ_f < 0.9%, Table S7, ESI†) in chloroform when compared to **P** (Φ_f = 75%).[32] Observed low Φ_f of **1–4AP** in chloroform could be attributed to alternate excited state decay pathways ($k_{nr} \approx k_{ISC} \gg k_r$) due to the incorporation of acetyl group(s).[16] Picosecond time-resolved fluorescence measurements of **1–4AP** in chloroform exhibit a short lifetime (τ_f = 1–2 ns) when monitored at respective emission maximum upon excitation at 375 nm (Fig. S8, ESI†). While **2–4AP** in chloroform shows a longer lifetime (*ca.* 3–5 ns) when monitored at a longer wavelength (500–550 nm) indicating the possibility of aggregation. Emission wavelength dependent excitation (Fig. S9, ESI†) in combination with concentration dependent emission (Fig. S10, ESI†) and excitation (Fig. S11, ESI†) spectra confirms the existence of ground state aggregate in **2-4AP** in $CHCl_3$.

In the crystalline state, **1–4AP** exhibited diverse colours ranging (Scheme 1, row III) from pale yellow–yellow–orange resulting in a red-shift of 100 nm in the absorption maximum of **4AP** when compared to **P** (Fig. S12, ESI†). Upon excitation at 350 nm, **1–4AP** exhibited a remarkable red-shift, for example 174 nm in the case of **4AP**, in the emission maximum when compared to **P** (Scheme 1, row IV and Fig. S12b and S13, ESI†).[32] Red-shift in the excimer-like fluorescence of **1–4AP** could be attributed to a combination of additional conjugation from acetyl groups and an increase in the extent of overlap between the adjacent pyrene moieties.[7] A significant red-shift in the excitation spectra of **1–4AP** when compared to the corresponding absorption spectra is indicative of ground state interaction between the vicinal pyrene units (Fig. S14, ESI†). A slip-stacked arrangement between the adjacent pyrene units in the crystalline **2**, **2′** and **2″AP** in combination with enhanced Φ_f, τ_f and k_r when compared to that in solution indicate the possibility of J-like aggregates and/or excimers of pyrene

(Table S7, ESI†).[33] Aggregate induced enhanced emission (AIEE) due to restricted motion of the flanking acetyl groups could also result in the enhanced fluorescence of the crystalline **2**, **2′** and **2″AP**.[35] Enhanced Φ_f in **3–4AP** could be attributed to a combination of AIE, ground state aggregation and cross-dipole arrangement of the adjacent pyrene moieties as reported earlier.[31,36] Among all the crystalline derivatives **1–4AP**, non-linear increase in the emission maximum of **3–4AP** could be a consequence of orbital overlap between the adjacent pyrene units from near-orthogonal arrangement.

In summary, we modulated the extent of π–π overlap between vicinal pyrene units through successive acylation. Unprecedented heteropolar dihydrogen contacts (sp^2 C–H···H–C sp^3) in organic crystals are established using QTAIM. Hirshfeld surface analysis is indicative of an increase in π–π interactions and a concomitant decrease in the σ–π interactions with an increase in the number of acetyl groups per pyrene unit. A combination of C–H···H–C, C–H···O and π–π interactions facilitate the transformation of sandwich herringbone packing of **P** to the herringbone arrangement in **1** and **2′AP**, the brickwork arrangement in **2** and **2″AP** and columnar stacks in **3–4AP**. A systematic decrease in the interplanar angle between the vicinal pyrene units could be attributed to the dramatic shift in the emission spectra (*ca.* 42–174 nm) of crystalline **1–4AP** when compared to pyrene. J-like aggregation and/or AIE in the crystal packing of **1–4AP** corroborates the moderately emissive blue–green–orange crystals. Efforts are progressing in our laboratory to correlate the photoconduction *vs.* crystal packing of acetylpyrene derivatives.

Authors dedicate this work to Professor M. V. George on the occasion of his 86th birthday. M. H. acknowledges the Science and Engineering Research Board (SERB) for the support of this work, SERB/F/0962. Authors thank Mr Alex P. Andrews for X-ray crystal structure analysis of **1–4AP**. S. K. R. and K. N. acknowledge the Council of Scientific and Industrial Research, India for the Research Fellowship. The authors gratefully acknowledge the anonymous reviewers for their valuable comments and suggestions to improve the quality of this manuscript.

Notes and references

1 M. D. Hollingsworth, *Science*, 2002, **295**, 2410–2413.
2 (*a*) J. D. Servaites, B. M. Savoie, J. B. Brink, T. J. Marks and M. A. Ratner, *Energy Environ. Sci.*, 2012, **5**, 8343–8350; (*b*) G. Raffy, D. Ray, C.-C. Chu, A. Del Guerzo and D. M. Bassani, *Angew. Chem., Int. Ed.*, 2011, **50**, 9584–9588; (*c*) B. Kahr, J. Freudenthal and E. Gunn, *Acc. Chem. Res.*, 2010, **43**, 684–692.
3 (*a*) D. J. Lipomi and Z. Bao, *Energy Environ. Sci.*, 2011, **4**, 3314–3328; (*b*) S. Varughese, *J. Mater. Chem. C*, 2014, **2**, 3499–3516; (*c*) J. E. Anthony, *Chem. Rev.*, 2006, **106**, 5028–5048; (*d*) T. Kawai, Y. Nakashima and M. Irie, *Adv. Mater.*, 2005, **17**, 309–314.
4 (*a*) B. Kippelen and J.-L. Bredas, *Energy Environ. Sci.*, 2009, **2**, 251–261; (*b*) G. R. Hutchison, M. A. Ratner and T. J. Marks, *J. Am. Chem. Soc.*, 2005, **127**, 16866–16881; (*c*) H. Moon, R. Zeis, E.-J. Borkent, C. Besnard, A. J. Lovinger, T. Siegrist, C. Kloc and Z. Bao, *J. Am. Chem. Soc.*, 2004, **126**, 15322–15323.
5 J. E. Anthony, J. S. Brooks, D. L. Eaton and S. R. Parkin, *J. Am. Chem. Soc.*, 2001, **123**, 9482–9483.
6 (*a*) Q. Feng, M. Wang, B. Dong, C. Xu, J. Zhao and H. Zhang, *CrystEngComm*, 2013, **15**, 3623–3629; (*b*) Y.-C. Chang, Y.-D. Chen, C.-H. Chen, Y.-S. Wen, J. T. Lin, H.-Y. Chen, M.-Y. Kuo and I. Chao, *J. Org. Chem.*, 2008, **73**, 4608–4614.
7 Q. Feng, M. Wang, B. Dong, J. He and C. Xu, *Cryst. Growth Des.*, 2013, **13**, 4418–4427.
8 T. Mutai, H. Satou and K. Araki, *Nat. Mater.*, 2005, **4**, 685–687.
9 (*a*) K. Nagura, S. Saito, H. Yusa, H. Yamawaki, H. Fujihisa, H. Sato, Y. Shimoikeda and S. Yamaguchi, *J. Am. Chem. Soc.*, 2013, **135**, 10322–10325; (*b*) X. Sun, X. Zhang, X. Li, S. Liu and G. Zhang, *J. Mater. Chem.*, 2012, **22**, 17332–17339.
10 H. Ito, M. Muromoto, S. Kurenuma, S. Ishizaka, N. Kitamura, H. Sato and T. Seki, *Nat. Commun.*, 2013, **4**, 2009.
11 S. Varghese and S. Das, *J. Phys. Chem. Lett.*, 2011, **2**, 863–873.
12 J. R. Lakowicz, *Principles of Fluorescence Spectroscopy*, Springer, New York, 3rd edn, 2006.
13 (*a*) R. T. Cheriya, K. Nagarajan and M. Hariharan, *J. Phys. Chem. C*, 2013, **117**, 3240–3248; (*b*) R. T. Cheriya, J. Joy, A. P. Alex, A. Shaji and M. Hariharan, *J. Phys. Chem. C*, 2012, **116**, 12489–12498.
14 R. T. Cheriya, A. R. Mallia and M. Hariharan, *Energy Environ. Sci.*, 2014, **7**, 1661–1669.
15 C. Friedel and J. M. Crafts, *J. Chem. Soc.*, 1877, **32**, 725–791.
16 Y. Niko, Y. Hiroshige, S. Kawauchi and G. Konishi, *J. Org. Chem.*, 2012, **77**, 3986–3996.
17 F. D. Lewis and J.-S. Yang, *J. Phys. Chem. B*, 1997, **101**, 1775–1781.
18 T. Hassheider, S. A. Benning, H.-S. Kitzerow, M.-F. Achard and H. Bock, *Angew. Chem., Int. Ed.*, 2001, **40**, 2060–2063.
19 (*a*) T. M. Figueira-Duarte and K. Müllen, *Chem. Rev.*, 2011, **111**, 7260–7314; (*b*) A. Hayer, V. de Halleux, A. Köhler, A. El-Garoughy, E. W. Meijer, J. Barberá, J. Tant, J. Levin, M. Lehmann, J. Gierschner, J. Cornil and Y. H. Geerts, *J. Phys. Chem. B*, 2006, **110**, 7653–7659.
20 G. R. Desiraju, *Acc. Chem. Res.*, 1996, **29**, 441–449.
21 S. Paliwal, S. Geib and C. S. Wilcox, *J. Am. Chem. Soc.*, 1994, **116**, 4497–4498.
22 J. Echeverria, G. Aullon, D. Danovich, S. Shaik and S. Alvarez, *Nat. Chem.*, 2011, **3**, 323–330.
23 E. V. Anslyn and D. A. Dougherty, *Modern Physical Organic Chemistry*, University Science Books, Sausalito, CA, 2006.
24 H. Vollmann, H. Becker, M. Corell and H. Streeck, *Justus Liebigs Ann. Chem.*, 1937, **531**, 1–159.
25 J. B. Birks, A. A. Kazzaz and T. A. King, *Proc. R. Soc. London, Ser. A*, 1966, **291**, 556–569.
26 A. Camerman and J. Trotter, *Acta Crystallogr.*, 1965, **18**, 636–643.
27 V. I. Bakhmutov, *Dihydrogen Bond: Principles, Experiments, and Applications*, John Wiley & Sons, Inc., Hoboken, New Jersey, 2008.
28 (*a*) R. F. W. Bader, *Atoms in Molecules: A Quantum Theory*, Oxford University Press, Oxford, U.K., 1990; (*b*) A. Volkov, P. Macchi, L. J. Farrugia, C. Gatti, P. R. Mallinson, T. Richter and T. Koritsanszky, *User Manual, vol. XD2006, a computer program package for multipole refinement, topological analysis of charge densities and evaluation of intermolecular energies from experimental or theoretical structure factors*, 2006 edn, User Manual, 2006.
29 D. J. Wolstenholme, J. Flogeras, F. N. Che, A. Decken and G. S. McGrady, *J. Am. Chem. Soc.*, 2013, **135**, 2439–2442.
30 S. K. Wolff, D. J. Grimwood, J. J. McKinnon, D. Jayatilaka and M. A. Spackman, *CrystalExplorer 3.0*, University of Western Australia, Perth, 2009, http://hirshfeldsurface.net/CrystalExplorer.
31 V. de Halleux, J. P. Calbert, P. Brocorens, J. Cornil, J. P. Declercq, J. L. Brédas and Y. Geerts, *Adv. Funct. Mater.*, 2004, **14**, 649–659.
32 R. Katoh, K. Suzuki, A. Furube, M. Kotani and K. Tokumaru, *J. Phys. Chem. C*, 2009, **113**, 2961–2965.
33 (*a*) F. C. Spano, *Acc. Chem. Res.*, 2010, **43**, 429–439; (*b*) J. Gierschner, L. Lüer, B. Milián-Medina, D. Oelkrug and H.-J. Egelhaaf, *J. Phys. Chem. Lett.*, 2013, **4**, 2686–2697; (*c*) U. Rösch, S. Yao, R. Wortmann and F. Würthner, *Angew. Chem., Int. Ed.*, 2006, **45**, 7026–7030.
34 L. Loots and L. J. Barbour, *CrystEngComm*, 2012, **14**, 300–304.
35 (*a*) Y. Hong, J. W. Y. Lam and B. Z. Tang, *Chem. Soc. Rev.*, 2011, **40**, 5361–5388; (*b*) S.-L. Tou, G.-J. Huang, P.-C. Chen, H.-T. Chang, J.-Y. Tsai and J.-S. Yang, *Chem. Commun.*, 2014, **50**, 620–622.
36 (*a*) M. Shimizu and T. Hiyama, *Chem. – Asian J.*, 2010, **5**, 1516–1531; (*b*) Z. Xie, B. Yang, F. Li, G. Cheng, L. Liu, G. Yang, H. Xu, L. Ye, M. Hanif, S. Liu, D. Ma and Y. Ma, *J. Am. Chem. Soc.*, 2005, **127**, 14152–14153.